Arch Clin Infect Dis. 2017 October; 12(4):e13823. doi: 10.5812/archcid.13823.
Published online 2017 September 23. **Research Article**

Lopinavir; A Potent Drug against Coronavirus Infection: Insight from Molecular Docking Study

Mohammad Reza Dayer,[1,*] Sara Taleb-Gassabi,[1] and Mohammad Saaid Dayer[2]

[1]Department of Biology, Faculty of Science, Shahid Chamran University of Ahvaz, Ahvaz, IR Iran
[2]Department of Parasitology and Medical Entomology, Tarbiat Modares University, Tehran

[*]*Corresponding author*: Mohammad Reza Dayer, Department of Biology, Faculty of Science, Shahid Chamran University of Ahvaz, Ahvaz, IR Iran. Tel: +98-6133331045, Fax: +98-6133331045, E-mail: mrdayer@scu.ac.ir

Received 2016 May 07; **Revised** 2017 May 22; **Accepted** 2017 September 19.

Abstract

Background: The severe acute respiratory syndrome (SARS) is a life threatening viral infection caused by a positive, single stranded RNA virus from the enveloped coronaviruse family. Associated with fever, cough, and respiratory complications, the illness causes more than 15% mortality worldwide. So far, there is no remedy for the illness except supportive treatments. However, the main viral proteinase has recently been regarded as a suitable target for drug design against SARS infection due to its vital role in polyproteins processing necessary for coronavirus reproduction.
Objectives: The present in silico study was designed to evaluate the effects of anti HIV-1 proteases inhibitors, approved for clinical applications by US FDA, on SARS proteinase inhibition.
Methods: In the present study, docking and molecular dynamic experiments were applied to examine the effect of inhibitors on coronavirus proteinase under physiological conditions of similar pH, temperature, and pressure in aqueous solution. Hex software version 5.1 and GROMACS 4.5.5 were used for docking analysis throughout this work.
Results: The calculated parameters such as RMSD, RMSF, MSD, dipole moment, diffusion coefficient, binding energy, and binding site similarity indicated effective binding of inhibitors to SARS proteinase resulting in their structural changes, which coincide with proteinase inhibition.
Conclusions: The inhibitory potency of HIV 1 protease inhibitors to cronovirus proteinase was as follows: LPV > RTV > APV > TPV > SQV. Lopinavir and Saquinavir were the most and the least powerful inhibitors of cronovirus proteinase, respectively.

Keywords: Severe Acute Respiratory Syndrome, Anti HIV-1 Protease Inhibitors, Lopinavir, Molecular Dynamic Simulation

1. Background

The agent of severe acute respiratory syndrome (SARS), the human coronavirus (HCoV), is an enveloped positive single stranded RNA virus from Coronaviridae family, which has a genome size of about 29.7 kb (1-4). Fever, cough, and progressive breath failure associated with respiratory complication are the main terrible manifestations of SARS infection. High prevalence of hospitalization and mortality risk (> 15%), in addition to the lack of prophylactic vaccines and therapeutic protocols, comprise serious challenges of SARS at times of global outbreaks (5-8). The genome of SARS encodes 2 polyproteins namely ppla and pplb, with molecular weights of 450 and 750 KD, respectively. These polyproteins are cleaved to different functional proteins of spike, membrane, envelop, nucleoprotein, replicase, and polymerase (9-11). This process is performed by a chymotrypsin-fold proteinase of 33KD molecular mass. This proteinase is called main protease (Mpro) or 3C-like protease (3CLpro) because of its similarity to protease picornavirus 3C in its folding and function (12-14).

As a homodimer with optimum activity at pH 7.5 and 42°C, the coronavirus Mpro, EC: 3.4.22.69, is highly conserved among Coronaviridae members exhibiting about 40% - 44% of sequence homology (15, 16). The Mpro has 3 structural domains; domain I (residues 8 - 101) and domain II (residues 102 - 184) both have beta barrel motifs representing chymotrypsin catalytic domain and domain III (residues 185 - 200) with a helical structure participates in dimerization of protein and active enzyme production (17, 18). Located at the interface between domains I and II, the 2 conserved residues His41 and Cys145 form the catalytic dyad of Mpro (2, 19, 20). Unlike other viral proteases, Mpro uses Cys residue of the catalytic dyad instead of Ser for nucleophilic attacks (16, 17).

Given its vital role in polyprotein processing and virus maturation, Mpro is considered to be a suitable target for viral inhibitor development as an approach toward SARS

treatment (21-23). On the other hand, HIV-1 protease inhibitors are widely reported to be able to deactivate Mpro and hence their nomination as potential drugs against SARS infection (24, 25).

This study has therefore been undertaken to study the molecular interaction of HIV-1 protease inhibitors with Mpro through docking/molecular dynamic (MD) experimentation in order to understand the underlining mechanisms to be used in designing more effective drugs for SARS infection.

2. Methods

Substrate Construction: It is well documented that Mpro may cleave polyproteins substrate at more than 10 conserved motif containing Leu-Gln↓ (Ser,Ala,Gly) sequences. This means that the preferred substrate should contain Leu at P2 and Gln at P1 position (see Figure 1: the cleavage site is indicated by↓) (25, 26).

Figure 1. Standard Nomenclature for Peptide Substrates in Which Amino Acid Residues are Denoted as Pn….P3P2P1↓P1'P2'P3'….Pn' with ↓ Represents the Hydrolysis site in Accordance

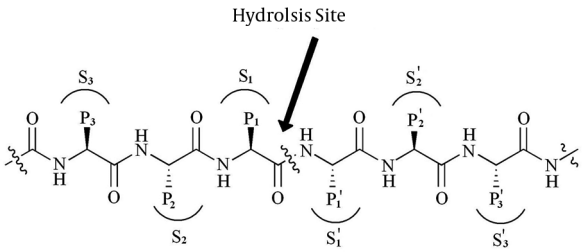

The counter groups on active site cavity are represent as Sn….S3S2S1↓S1'S2'S3'….Sn'.

Figure 1 represents standard nomenclatures for polypeptide substrates and the corresponding binding site cavity (27). In order to find the enzyme binding site, we constructed a substrate with TVLQSGFR sequence in Argus-Lab 4.0.1 Software (http://www.arguslab.com) and docked this substrate to optimized coordinate structure of Mpro in Hex software version 5.1 (http://www.loria.fr/~ ritchied/hex/) (28).

Enzyme coordinate structure: the crystal structure of Mpro with PDBID of 1UK3 was used as a starting structure throughout this study. Obtained by the X-Ray diffraction method and refined at the resolutions of 2.4Å, the structure was retrieved from the protein data bank (http://www.rcsb.org/pdb). The structure was optimized to lower than 300 KJ/Mol of total energy using the GROMACS software via the same method used in MD settings. A short equilibration run of MD was then followed for 2ns at 37°C, neutral pH, and 1 atmosphere of pressure. After removing the PBC effects, solvent, as well as other heteroatoms, the structure was then saved in the PDB format.

Docking experiments: approved inhibitors of HIV-1 protease including tipranavir (TPV), saquinavir (SQV), ritonavir (RTV), nelfinavir (NFV), lopinavir (LPV), indinavir (IDV), darunavir (DAR), atazanavir (ATV), and amprenavir (APV) were constructed and optimized in the ArgusLab software (Figure 2).

The structures of the substrate and inhibitors were docked to the optimized structure of Mpro in the Hex software version 5.1 (http://www.loria.fr/~ ritchied/hex/). The blind docking algorithm was used to study the physical fitness of inhibitors to their binding site. Docking results were then scored based on their energy and the first 200 solutions were collected and statistically analyzed. The binding site residues of each ligand were extracted by the Argus-Lab software separately.

2.1. Molecular Dynamic Simulation Setting

The best enzyme-inhibitors complex with maximum binding energy was selected for MD simulations. These complexes were placed in the center of a rectangular box (6.97 × 8.95 × 8.71 nm) filled with SPC water molecules. Molecular dynamic simulations were performed using the double-precision MPI version of GROMACS 4.5.5 installed on UBUNTU version 14.04 and 53A5 force field. The net charge of simulated systems was analyzed by preprocessor engine of GROMACS package. System neutralization was done by adding an equivalent number of positive ions of sodium. Total energy of hydrogen atoms, ions, and water molecules were minimized in 1500 steps using the steepest descent method to under 300 kJ/mol. The other MD setting was as reported before at a neutral pH (29, 30).

3. Results

In order to determine the binding energy and fitness of the inhibitors to the enzyme active site and to extract their preferred binding site, we carried out a serial docking experiment as mentioned above, each in triplicate. Our data (Table 1) indicated that binding energies of inhibitors fitness are as follow: LPV > SQV > TPV > RTV > IDV > ATV > DAR > NFV > APV. To extract the binding site residues of each inhibitor, the best corresponding complex was analyzed by Argus-Lab 4.0.1 software and the amino acid content was compared to that of the substrate. The amino acid content similarity of binding sites of each inhibitor to the substrate was calculated and presented in Table 1. As tabulated, given a high similarity between the substrate and the inhibitors' binding sites, drugs such as LPV, APV, RTV,

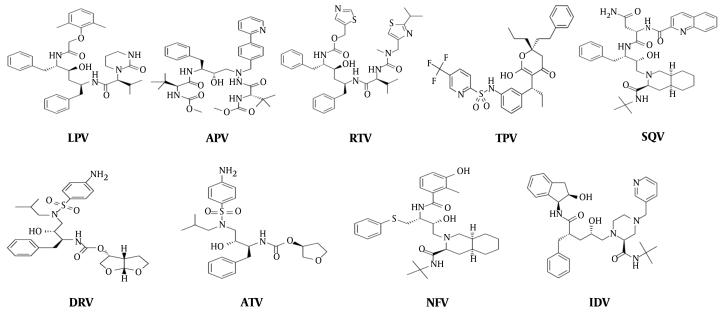

Figure 2. Chemical Structures of HIV-1 Protease Inhibitors

TPV, and SQV represent the strongest rivals of the polyproteins to bond to the enzyme active site. Therefore, we selected LPV, APV, RTV, TPV, and SQV as potent inhibitors for further experimentation. No significant correlation was found between binding energies (as in Table 1) and molecular weights of inhibitors (data not shown).

Table 1. Binding Energy and Binding Site Similarities were Extracted from Docking Experiments Using the Hex software[a]

Inhibitor	Binding Energy[b]	Binding Site Similarity, %	MW
LPV	-413.99 ± 29.31	66.67	628.81
APV	-331.23 ± 20.26	55.56	505.62
RTV	-381.93 ± 43.17	55.56	720.94
TPV	-398.55 ± 43.36	51.85	602.66
SQV	-400.87 ± 27.66	51.85	670.84
DAR	-360.75 ± 31.22	33.33	547.66
ATV	-361.45 ± 38.45	33.33	704.85
NFV	-354.25 ± 29.88	0	567.78
IDV	-372.61 ± 30.21	0	613.79

[a]The binding site contents were extracted by the ArgusLab software.
[b]Values are expressed as mean ± SD.

Figure 3 illustrates the locations of inhibitors binding sits in contrast to the substrate binding site to provide a holistic understanding on the subject.

Root mean square displacement (RMSD) of MD experiments (Figure 4) indicates that 50ns period of simulation completely covers all changes induced by inhibitors in the Mpro structure. This figure conveys that our systems experience structural alterations during simulation as manifested in increased RMSD to about 1 nanometer. The extents of these alterations are high enough to be attributed to all structural alterations induced by inhibitors. The final 30ns trend of RMSD curve is indicative of the prevalence of the equilibration state with less than 0.2 nm fluctuation in RMSD curve.

Structural flexibility is one of the important physical properties that affect protein conformation and function. Whereas high increase in kinetics energy and protein flexibility can disrupt non covalent interactions as in thermal denaturation; a sharp decrease in flexibility can also cause protein denaturation as seen in cold denaturation. Therefore, proteins need an essential amount of flexibility to carry out their native function at physiological conditions. In this context, an inhibitor by binding to a protein can alter its flexibility and decrease its enzymatic activity. As indicated in Figure 5A and 5B, LPV reduces Mpro flexibility more effectively than TPV and other inhibitors. This may be attributed to the tighter attachment of LPV to Mpro enzyme, which results in a stronger inhibitory effect.

The g_dipol command in GROMACS package calculates the dipole moment of inhibitors in the Debye unit during the simulation period (Figure 6). The dipole moment of an inhibitor is a physical property determined by their chemical structure and affected by surrounding conditions of solvent, solutes, and temperature. The dipole moment provides a good index for inhibitor polarity during simulation. Figure 6 indicates that LPV and SQV show the lowest and the highest dipole moments, respectively. The lower dipole moment for LPV conveys its more hydrophobic property that facilitates its interaction with the hydrophobic core of Mpro compared to other inhibitors.

Diffusion constant for inhibitors during simulation is another useful parameter, which indicates the extent to which inhibitors penetrate inside Mpro protein. This parameter could be pulled out from the slope of MSD curve obtained by g_msd commands of the GROMACS package (Figure 7). As expected from the dipole moment, LPV and SQV showed the highest and the lowest diffusion constants, respectively. This finding reconfirms the hypothetic higher inhibitory potency of LPV.

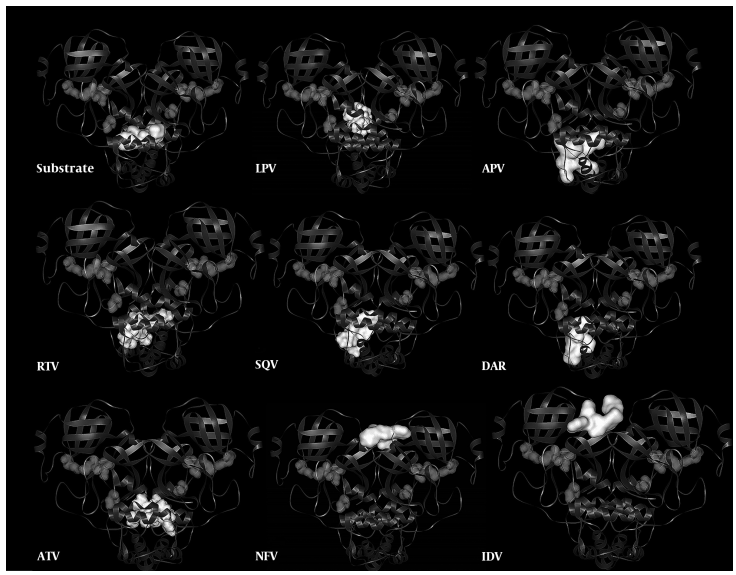

Figure 3. Graphical Representation of Inhibitors Binding to the Enzyme Tertiary Structure

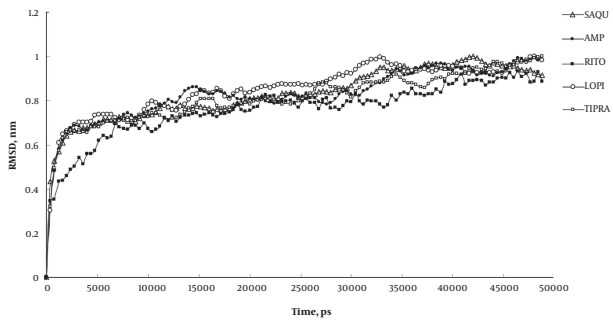

Figure 4. RMSD Curve for Mpro During 50ns Simulation Period in Contrast to Its Initial State Obtained from Simulation at 37°C, Neutral pH and 1 Atmosphere of Pressure in SPC Water Box.

4. Discussion

Efforts are globally underway to create an efficient vaccine or drug for prevention or treatment of the SARS infection (31-33). In this context, many reports showed that Mpro is an ideal target for drug design and development (34-36). The well-characterized inhibitors of Mpro can be classified into 2 classes based on their chemical structures. The first class includes a peptide chain with an ending reactive group. This kind of inhibitor fits the catalytic site of the enzyme by making a covalent link with Cys145 via its reactive group and therefore it blocks the substrate entry to the active site (37, 38).

The 2nd class involves small organic compounds that bind to the enzyme active site groups and/or to groups in its vicinities so that they competitively prevent a substrate entrance to the active site cavity. Anti-protease inhibitors approved for viral infection treatment are interesting examples in this connection. Recently, these inhibitors are screened for their capability to inhibit Mpro and treat SARS infection using in vivo, in vitro, and in silico experiments (34-39). The clinical trial of LPV showed a significant decrease in virus titer, reduced rate of death, and improved clinical recovery (40-42). In this direction, it deemed appropriate to study in detail the molecular interactions between Mpro coordinate structure and HIV-1 protease inhibitors using femtosecond snapshots of MD simulations trajectories. Accordingly, this study primarily aimed to draw a detailed prospective from HIV-1 protease inhibitors-Mpro complexes to help design more effective inhibitors for the SARS infectious.

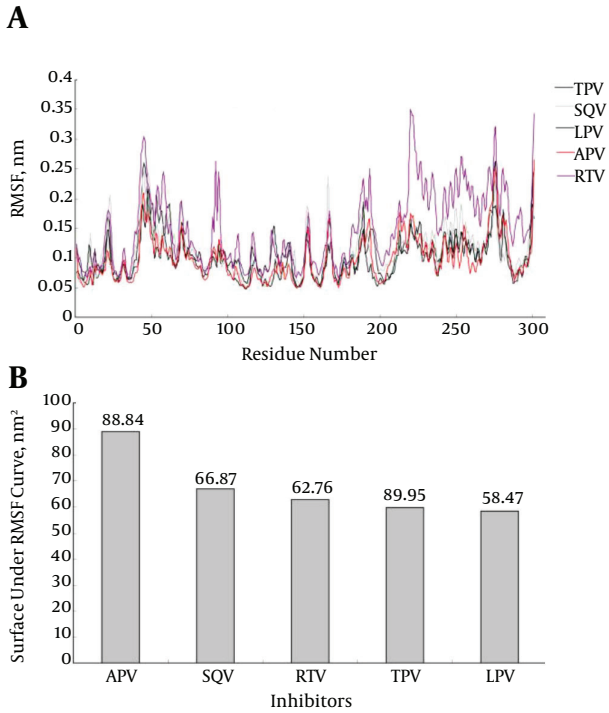

Figure 5. A, RMSF Curve for Alpha Carbons of Mpro During the Simulation Period of 50ns at pH7, 37°C, and 1 Atmosphere of Pressure; B, Surface Under Each of RMSF Curves Obtained by Integrating the Curves.

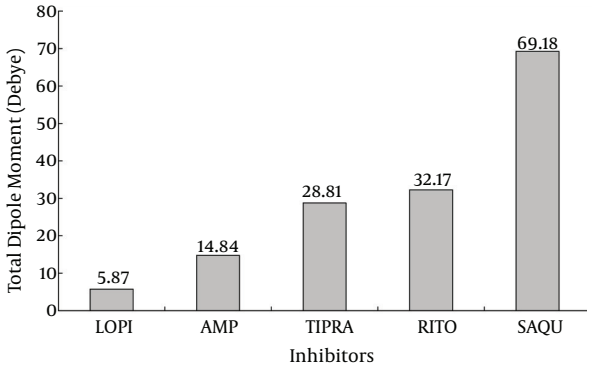

Figure 6. Total Dipole Moment for Inhibitors Calculated in Simulated Systems Using g_dipol Command

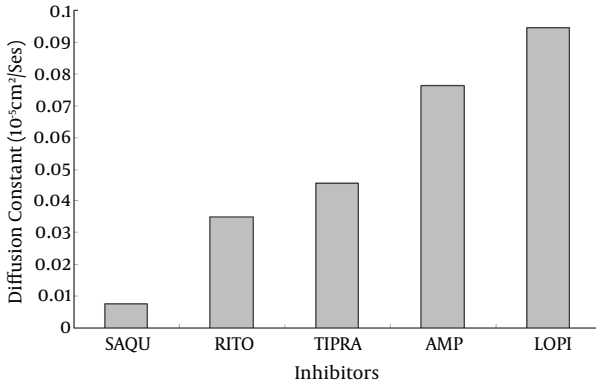

Figure 7. Diffusion Coefficient of Inhibitors Inside Mpro Calculated from Mean Square Displacement Curve for Inhibitors Extracted from Trajectory File by g_msd Command

Our data indicated that among the 9 tested inhibitors, 5 could bind to sites that resemble their preferred active sites with more than 50% similarities (Table 1). Our structural inspection revealed that there are 2 factors affecting inhibitors' binding efficacy. The first factor is the extent of similarity of the inhibitor specific binding site to Mpro active site, e.g. the more similarity exists the more effective inhibition of enzyme occurs. The 2nd important factor is Mpro structural complexity and spatial accommodation required for inhibitors binding. Therefore, adopting a complex structure of maximum similarity to its specific binding site upon interaction with Mpro, LPV causes maximum decrease in RMSF (Figure 5B) and maximum inhibitory effect.

Although, LPV showed the highest binding energy (-413.99 ± 29.31KJ/Mol) and maximum similarity (66.67%) to the enzyme active site, no significant correlation was found between binding energy and binding site similarity or molecular weight for other tested inhibitors. These findings reveal that the binding energy of inhibitors is not merely determined by binding site similarity or by inhibitors molecular weight. Instead, it is likely determined by the mode of spatial binding of inhibitors to enzyme binding site and the arrangement of their functional groups to their counter groups on the enzyme active site.

The same change in RMSD curves of inhibitors (Figure 4) assures that the systems experience equal conformational changes; therefore, it could be used for a comparative study. As indicated, only LPV reduces the total RMSF of protein to its minimum amount, which means that LPV is the strongest inhibitor of Mpro (42, 43). Figure 5A plots the average fluctuation of each alpha carbon during 50ns period of simulation. Alpha carbons, with high fluctuation comprise hot points or flexible points for Mpro protein. The high fluctuating curve for Mpro, in the presence of certain inhibitors, indicates that the inhibitor does not restrict or limit protein flexibility (weak inhibitor). Conversely, a strong inhibitor is expected to restrict enzyme flexibility with lower average of fluctuation for the enzyme active site (Figure 5B). Inhibitor hydrophobicity was calculated in situ as a dipole moment of inhibitors by g_-

dipol command of the GROMACS software. According to these data (Figure 6), in contrast to other inhibitors, LPV expresses more hydrophobic property. This results in effective binding of LPV to Mpro and therefore, a steeper decrease in RMSF of LPV (Figure 5B). As expected, among other inhibitors, LPV shows the highest diffusion constant, which reconfirm its efficient inhibition character (Figure 7).

While RMSF and dipole moment are inversely proportional to inhibitory potency and diffusion coefficient of inhibitors, the hydrogen bonds formed between binding site groups and the level of their residual similarity are directly proportional to inhibitory power (Table 2). Each set of data were normalized and averaged for each inhibitor as an inhibitory index. The data show that inhibitory potency or the index for inhibitors are as follow: LPV < RTV < APV < TPV < SQV, in which LPV and SQV have the highest and the lowest potency for Mpro inhibition.

Table 2. Docking and MD Parameters Obtained for Inhibitors and Calculated as Inhibitory Indexes

	APV	SQV	RTV	TPV	LPV
RMSF	88.83	66.87	62.76	59.94	58.46
Dipole Moment	14.83	69.18	32.17	28.81	5.87
Binding site Hydrophobicity	13.4	7.2	13.3	16.4	21.7
Diffusion Coefficient	0.076	0.007	0.035	0.045	0.094
H.Bond	3	1	6	2	5
Binding Site Similarity	55.56	51.85	55.56	51.58	66.67
Shape Energy	-331.23	-400.87	-381.93	-398.55	-413.99
Index	0.58	0.48	0.64	0.51	0.76

Reports on in vivo and in vitro applications of LPV in SARS treatment provided evidence that LPV and RTV may improve the Ribavarin effect on SARS infections in a dose dependent manner and reduce the death rate by about 20% - 30% (43, 44). Also, NFV, an anti HIV-1 protease, showed to prevent coronavirus replication and limit its cytotoxic effect on host cells (31-33, 44).

4.1. Conclusions

Taking into consideration our findings and the available clinical evidences on the usefulness of anti HIV-1 protease inhibitors for SARS infection treatment, tested inhibitors can be ranked based on their inhibitory potency as follows: LPV < RTV < APV < TPV < SQV. In the absence of even a single effective drug for SARS treatment, our findings represent a promising pharmaceutical perspective for the disease therapy via Mpro inhibition.

References

1. Adedeji AO, Sarafianos SG. Antiviral drugs specific for coronaviruses in preclinical development. *Curr Opin Virol*. 2014;**8**:45–53. doi: 10.1016/j.coviro.2014.06.002. [PubMed: 24997250].
2. Rota PA, Oberste MS, Monroe SS, Nix WA, Campagnoli R, Icenogle JP, et al. Characterization of a novel coronavirus associated with severe acute respiratory syndrome. *Science*. 2003;**300**(5624):1394–9. doi: 10.1126/science.1085952. [PubMed: 12730500].
3. Berger A, Drosten C, Doerr HW, Sturmer M, Preiser W. Severe acute respiratory syndrome (SARS)–paradigm of an emerging viral infection. *J Clin Virol*. 2004;**29**(1):13–22. [PubMed: 14675864].
4. Liang W, McLaws ML, Liu M, Mi J, Chan DK. Hindsight: a re-analysis of the severe acute respiratory syndrome outbreak in Beijing. *Public Health*. 2007;**121**(10):725–33. doi: 10.1016/j.puhe.2007.02.023. [PubMed: 17555781].
5. Shigeta S, Yamase T. Current status of anti-SARS agents. *Antivir Chem Chemother*. 2005;**16**(1):23–31. doi: 10.1177/095632020501600103. [PubMed: 15739619].
6. Cheng PK, Wong DA, Tong LK, Ip SM, Lo AC, Lau CS, et al. Viral shedding patterns of coronavirus in patients with probable severe acute respiratory syndrome. *Lancet*. 2004;**363**(9422):1699–700. doi: 10.1016/S0140-6736(04)16255-7. [PubMed: 15158632].
7. Dwosh HA, Hong HH, Austgarden D, Herman S, Schabas R. Identification and containment of an outbreak of SARS in a community hospital. *Can Med Assoc J*. 2003;**168**(11):1415–20.
8. Zhang XW, Yap YL. Exploring the binding mechanism of the main proteinase in SARS-associated coronavirus and its implication to anti-SARS drug design. *Bioorg Med Chem*. 2004;**12**(9):2219–23. doi: 10.1016/j.bmc.2004.02.015. [PubMed: 15080921].
9. Groneberg DA, Hilgenfeld R, Zabel P. Molecular mechanisms of severe acute respiratory syndrome (SARS). *Respir Res*. 2005;**6**:8. doi: 10.1186/1465-9921-6-8. [PubMed: 15661082].
10. Lin PY, Chou CY, Chang HC, Hsu WC, Chang GG. Correlation between dissociation and catalysis of SARS-CoV main protease. *Arch Biochem Biophys*. 2008;**472**(1):34–42. doi: 10.1016/j.abb.2008.01.023. [PubMed: 18275836].
11. Jacobs J, Grum-Tokars V, Zhou Y, Turlington M, Saldanha SA, Chase P, et al. Discovery, synthesis, and structure-based optimization of a series of N-(tert-butyl)-2-(N-arylamido)-2-(pyridin-3-yl) acetamides (ML188) as potent noncovalent small molecule inhibitors of the severe acute respiratory syndrome coronavirus (SARS-CoV) 3CL protease. *J Med Chem*. 2013;**56**(2):534–46. doi: 10.1021/jm301580n. [PubMed: 23231439].
12. Fan K, Wei P, Feng Q, Chen S, Huang C, Ma L, et al. Biosynthesis, purification, and substrate specificity of severe acute respiratory syndrome coronavirus 3C-like proteinase. *J Biol Chem*. 2004;**279**(3):1637–42.
13. Huang C, Wei P, Fan K, Liu Y, Lai L. 3C-like proteinase from SARS coronavirus catalyzes substrate hydrolysis by a general base mechanism. *Biochemistry*. 2004;**43**(15):4568–74. doi: 10.1021/bi036022q. [PubMed: 15078103].
14. Lin CW, Tsai CH, Tsai FJ, Chen PJ, Lai CC, Wan L, et al. Characterization of trans- and cis-cleavage activity of the SARS coronavirus 3CLpro protease: basis for the in vitro screening of anti-SARS drugs. *FEBS Lett*. 2004;**574**(1-3):131–7. doi: 10.1016/j.febslet.2004.08.017. [PubMed: 15358553].
15. Ziebuhr J. Molecular biology of severe acute respiratory syndrome coronavirus. *Curr Opin Microbiol*. 2004;**7**(4):412–9. doi: 10.1016/j.mib.2004.06.007. [PubMed: 15358261].
16. Anand K, Palm GJ, Mesters JR, Siddell SG, Ziebuhr J, Hilgenfeld R. Structure of coronavirus main proteinase reveals combination of a chymotrypsin fold with an extra alpha-helical domain. *EMBO J*. 2002;**21**(13):3213–24. doi: 10.1093/emboj/cdf327. [PubMed: 12093723].

17. Bacha U, Barrila J, Velazquez-Campoy A, Leavitt SA, Freire E. Identification of novel inhibitors of the SARS coronavirus main protease 3CLpro. *Biochemistry*. 2004;**43**(17):4906–12. doi: 10.1021/bi0361766. [PubMed: 15109248].
18. Zhang XW, Yap YL. Old drugs as lead compounds for a new disease? Binding analysis of SARS coronavirus main proteinase with HIV, psychotic and parasite drugs. *Bioorg Med Chem*. 2004;**12**(10):2517–21. doi: 10.1016/j.bmc.2004.03.035. [PubMed: 15110833].
19. Chan KS, Lai ST, Chu CM, Tsui E, Tam CY, Wong MML, et al. Treatment of severe acute respiratory syndrome with lopinavir/ritonavir: a multicentre retrospective matched cohort study. *Hong Kong Med J*. 2003.
20. Fan K, Ma L, Han X, Liang H, Wei P, Liu Y, et al. The substrate specificity of SARS coronavirus 3C-like proteinase. *Biochem Biophys Res Commun*. 2005;**329**(3):934–40. doi: 10.1016/j.bbrc.2005.02.061. [PubMed: 15752746].
21. Ahn TY, Kuo CJ, Liu HG, Ha DC, Liang PH, Jung YS. Synthesis and Evaluation of Benzoquinolinone Derivatives as SARS-CoV 3CL Protease Inhibitors. *Bull Korean Chem Soc*. 2010;**31**(1):87–91. doi: 10.5012/bkcs.2010.31.01.087.
22. Liang PH. Characterization and inhibition of SARS-coronavirus main protease. *Curr Top Med Chem*. 2006;**6**(4):361–76. [PubMed: 16611148].
23. Anand K, Ziebuhr J, Wadhwani P, Mesters JR, Hilgenfeld R. Coronavirus main proteinase (3CLpro) structure: basis for design of anti-SARS drugs. *Science*. 2003;**300**(5626):1763–7. doi: 10.1126/science.1085658. [PubMed: 12746549].
24. Yang H, Yang M, Ding Y, Liu Y, Lou Z, Zhou Z, et al. The crystal structures of severe acute respiratory syndrome virus main protease and its complex with an inhibitor. *Proc Natl Acad Sci U S A*. 2003;**100**(23):13190–5. doi: 10.1073/pnas.1835675100. [PubMed: 14585926].
25. Zhao Q, Weber E, Yang H. Recent developments on coronavirus main protease/3C like protease inhibitors. *Recent Pat Antiinfect Drug Discov*. 2013;**8**(2):150–6. [PubMed: 23879823].
26. Kim Y, Lovell S, Tiew KC, Mandadapu SR, Alliston KR, Battaile KP, et al. Broad-spectrum antivirals against 3C or 3C-like proteases of picornaviruses, noroviruses, and coronaviruses. *J Virol*. 2012;**86**(21):11754–62. doi: 10.1128/JVI.01348-12. [PubMed: 22915796].
27. Brik A, Wong CH. HIV-1 protease: mechanism and drug discovery. *Org Biomol Chem*. 2003;**1**(1):5–14. [PubMed: 12929379].
28. Thompson MA. Molecular docking using ArgusLab, an efficient shape-based search algorithm and the AScore scoring function. *ACS meeting*. Philadelphia. 2004. 42 p.
29. Mukherjee P, Shah F, Desai P, Avery M. Inhibitors of SARS-3CLpro: virtual screening, biological evaluation, and molecular dynamics simulation studies. *J Chem Inf Model*. 2011;**51**(6):1376–92. doi: 10.1021/ci1004916. [PubMed: 21604711].
30. Dayer MR, Ghayour O, Dayer MS. Mechanism of the bell-shaped profile of ribonuclease a activity: molecular dynamic approach. *Protein J*. 2012;**31**(7):573–9. doi: 10.1007/s10930-012-9435-4. [PubMed: 22851207].
31. Chang CK, Jeyachandran S, Hu NJ, Liu CL, Lin SY, Wang YS, et al. Structure-based virtual screening and experimental validation of the discovery of inhibitors targeted towards the human coronavirus nucleocapsid protein. *Mol Biosyst*. 2016;**12**(1):59–66. doi: 10.1039/c5mb00582e. [PubMed: 26542199].
32. Peters HL, Ku TC, Seley-Radtke KL. Flexibility as a Strategy in Nucleoside Antiviral Drug Design. *Curr Med Chem*. 2015;**22**(34):3910–21. [PubMed: 26282942].
33. Gross AE, Bryson ML. Oral Ribavirin for the Treatment of Noninfluenza Respiratory Viral Infections: A Systematic Review. *Ann Pharmacother*. 2015;**49**(10):1125–35. doi: 10.1177/1060028015597449. [PubMed: 26228937].
34. Kim Y, Shivanna V, Narayanan S, Prior AM, Weerasekara S, Hua DH, et al. Broad-spectrum inhibitors against 3C-like proteases of feline coronaviruses and feline caliciviruses. *J Virol*. 2015;**89**(9):4942–50. doi: 10.1128/JVI.03688-14. [PubMed: 25694593].
35. Berry M, Fielding BC, Gamieldien J. Potential Broad Spectrum Inhibitors of the Coronavirus 3CLpro: A Virtual Screening and Structure-Based Drug Design Study. *Viruses*. 2015;**7**(12):6642–60. doi: 10.3390/v7122963. [PubMed: 26694449].
36. St John SE, Therkelsen MD, Nyalapatla PR, Osswald HL, Ghosh AK, Mesecar AD. X-ray structure and inhibition of the feline infectious peritonitis virus 3C-like protease: Structural implications for drug design. *Bioorg Med Chem Lett*. 2015;**25**(22):5072–7. doi: 10.1016/j.bmcl.2015.10.023. [PubMed: 26592814].
37. Zhao Q, Weber E, Yang H. Drug targets for rational design against emerging coronaviruses. *Infect Disord Drug Targets*. 2013;**13**(2):116–27. [PubMed: 23895136].
38. Prior AM, Kim Y, Weerasekara S, Moroze M, Alliston KR, Uy RA, et al. Design, synthesis, and bioevaluation of viral 3C and 3C-like protease inhibitors. *Bioorg Med Chem Lett*. 2013;**23**(23):6317–20. doi: 10.1016/j.bmcl.2013.09.070. [PubMed: 24125888].
39. Chu CM. Role of lopinavir/ritonavir in the treatment of SARS: initial virological and clinical findings. *Thorax*. 2004;**59**(3):252–6. doi: 10.1136/thorax.2003.012658.
40. Yamamoto N, Yang R, Yoshinaka Y, Amari S, Nakano T, Cinatl J, et al. HIV protease inhibitor nelfinavir inhibits replication of SARS-associated coronavirus. *Biochem Biophys Res Commun*. 2004;**318**(3):719–25. doi: 10.1016/j.bbrc.2004.04.083. [PubMed: 15144898].
41. Peters HL, Jochmans D, de Wilde AH, Posthuma CC, Snijder EJ, Neyts J, et al. Design, synthesis and evaluation of a series of acyclic fleximer nucleoside analogues with anti-coronavirus activity. *Bioorg Med Chem Lett*. 2015;**25**(15):2923–6. doi: 10.1016/j.bmcl.2015.05.039. [PubMed: 26048809].
42. Dayer MR, Dayer MS, Ghayour O. Dynamic behavior of rat phosphoenolpyruvate carboxykinase inhibitors: new mechanism for enzyme inhibition. *Protein J*. 2013;**32**(4):253–8. doi: 10.1007/s10930-013-9481-6. [PubMed: 23532540].
43. Nagel ZD, Meadows CW, Dong M, Bahnson BJ, Klinman JP. Active site hydrophobic residues impact hydrogen tunneling differently in a thermophilic alcohol dehydrogenase at optimal versus nonoptimal temperatures. *Biochemistry*. 2012;**51**(20):4147–56.
44. Momattin H, Mohammed K, Zumla A, Memish ZA, Al-Tawfiq JA. Therapeutic options for Middle East respiratory syndrome coronavirus (MERS-CoV)–possible lessons from a systematic review of SARS-CoV therapy. *Int J Infect Dis*. 2013;**17**(10):e792–8.